Clin. Lab. 2024;70:XXX-XXX


## ORIGINAL ARTICLE

# Identification of Potential Biomarkers Associated with Spermatogenesis in Azoospermia

ChaoCheng Li *, MengYu Li *, YaXing Liu, Jian Li, YaRu Zhang, Hui Wang, YongSheng Zhang, Bin Jia

* *These authors contributed equally to this work*
*College of Animal Science and Technology, Shihezi University, Shihezi City, Xinjiang Uighur Autonomous Region, China*

**SUMMARY**

***Background:*** **Azoospermia, characterized by the absence of spermatozoa in the ejaculate, affects approximately 1% of all men and 10 - 15% of infertile males, representing the most severe form of male infertility. It is classified into obstructive azoospermia (OA) and nonobstructive azoospermia (NOA), with the latter often resulting from unexplained failures in spermatogenesis. This study endeavored to clarify the molecular underpinnings of spermatogenesis in NOA and to identify viable therapeutic targets.**

***Methods:*** **We analyzed expression data from NOA and normal spermatogenesis samples obtained from the GEO database. Differential expression analysis was performed to identify differentially expressed genes (DEGs). We then intersected these DEGs with genes known to be related to spermatogenesis to pinpoint spermatogenesis-related DEGs specific to NOA. Subsequent analyses, including gene ontology (GO) and Kyoto encyclopedia of genes and genomes (KEGG) pathway enrichments, aimed to elucidate potential signaling pathways involved. A protein-protein interaction (PPI) network was constructed to highlight hub genes, whose diagnostic potential was assessed by using ROC curve analysis. Additionally, miRNA and transcription factor (TF) regulatory network for hub genes were analyzed. The efficacy of identified hub genes as biomarkers was validated through RT-qPCR and Western blotting in a mouse model of NOA.**

***Results:*** **This study identified 68 NOV-specific spermatogenesis-related genes. Enrichment analyses in GO and KEGG pathways highlighted their involvement in cellular processes related to reproduction in multicellular organism and endocrine and other factor-regulated calcium reabsorption. Seven hub genes were identified, with ROC curve analysis affirming their significant diagnostic value. Constructed networks revealed intricate interactions among miRNAs, hub genes, and TFs.**

***Conclusions:*** **We identified seven hub genes (CATSPER1, CATSPER3, CATSPER4, CATSPERG, OAZ3, ODF1, and SUN5) significantly associated with spermatogenesis in NOA, demonstrating their potential as biomarkers for diagnosing and monitoring the disease.**

**(Clin. Lab. 2024;70:xx-xx. DOI: 10.7754/Clin.Lab.2024.240541)**

**Correspondence:**
Bin Jia
College of Animal Science and Technology
Shihezi University
No. 221, North 4th Road
Shihezi City
Xinjiang Uighur Autonomous Region, 832000
China
Email: jiabin@shzu.edu.cn

Manuscript accepted July 3, 2024

**KEYWORDS**

nonobstructive azoospermia, spermatogenesis, diagnosis genes

## INTRODUCTION

Azoospermia, the absence of sperm in ejaculated semen, accounts for approximately 10% - 15% of the male infertility cases [1]. Non-obstructive azoospermia

(NOA), distinguished from obstructive azoospermia (OA) by the absence of blockages in the vas deferens, represents the most severe form of azoospermia [2]. It primarily results from testicular dysfunction or abnormalities within the hypothalamic/pituitary axis, leading to negligible sperm production or a complete inability to produce sperm. The pathogenesis of NOA is complex, with known causes including sex chromosome abnormalities, cryptorchidism, translocations, Y chromosome microdeletions, and other genetic disorders-implicated intesticular failure [2,3]. Despite these insights, the origins of NOA remain unidentified in up to 73% of the cases [4].

Spermatogenesis is an extremely complex process of cellular differentiation, with over 2,300 genes involved in regulating the development and maturation of germ cells [5]. This process encompasses the maintenance of spermatogonial stem cells, preparation for differentiation, meiosis, and sperm production. Any changes in the testicular microenvironment can adversely affect sperm production and fertility [6]. However, the pathogenesis of NOA remains largely elusive, presenting substantial challenges in treatment [7]. Thus, delineating the molecular underpinnings of spermatogenesis, identifying spermatogenesis-related genes, and developing diagnostic markers and therapeutic targets are imperative for advancing NOA treatment and patient care.

Given the pivotal role of spermatogenesis in NOA progression, this study aimed to uncover genes associated with spermatogenesis in the context of NOA. Identifying these genes will not only enhance our understanding of NOA's biological mechanisms but also pave the way for novel diagnostic and therapeutic strategies for affected individuals.

## MATERIALS AND METHODS

### Data source

Expression data from microarray analysis for non-obstructive azoospermia (NOA) and corresponding controls were retrieved from the Gene Expression Omnibus (GEO) repository, specifically datasets GSE45885 and GSE145467. The former, encompassing 27 NOA specimens and 4 controls, served as the training set, whereas the latter, comprising 10 NOA specimens alongside 10 controls, functioned as the validation set. Additionally, a compilation of genes implicated in spermatogenesis was sourced from entry GO:0007283 in the Gene Ontology (GO) database.

### Differential expression analysis

Normalized microarray data were subjected to analysis using R software, with the 'limma' package facilitating the identification of differentially expressed genes (DEGs) between NOA cases and controls, adhering to thresholds of $|logFC| > 1$ and adjusted p-value $< 0.05$ for significance. Visual representation of DEGs was achieved through volcano plots, and expression patterns of the top deregulated DEGs were illustrated via heatmaps, both generated in R.

### Functional annotation and pathway enrichment analysis

Overlap genes between DEGs and spermatogenesis-related genes was determined by using Venn diagram analysis. Subsequent GO and KEGG pathway enrichment analyses were performed with the clusterProfiler package, focusing on biological processes (BP), molecular functions (MF), and cellular components (CC), where terms with an FDR $< 0.05$ were deemed significantly enriched [8,9].

### PPI network construction

The construction of the protein-protein interaction (PPI) network utilized the STRING database [10], and visualization was accomplished with Cytoscape software, incorporating the molecular complex detection (MCODE) plugin to identify significant modules [11,12].

### Evaluation and validation of diagnostic performance of hub genes

The diagnostic potential of hub genes was assessed through ROC curve analysis, using *pROC* package [13] to evaluate. The area under the curve (AUC) can evaluate the accuracy of hub genes and provides a basis for evaluating the diagnostic performance of hub genes. The hub genes are considered to have predictive value, with AUC values over 0.7. The higher the AUC value, the higher specificity and sensitivity.

### Interaction and GSEA analysis of hub genes

Spearman correlation analysis for hub genes was executed with the “ggpubr” package. Gene set enrichment analysis (GSEA) explored biological process variations across different gene expression levels, employing the HALLMARK gene set from the MSigDB database and the Org.Hs.eg.db package for GSEA, with significance set at adjusted p-value $< 0.05$.

### Multi-factor regulation network construction

To further understand the regulation of hub genes, the predictions on the transcription factors (TFs) and microRNAs (miRNAs) associated with hub genes utilized miRNet database [14]. An integrated regulatory network was then visualized using Cytoscape software, facilitating a deeper understanding of hub gene regulation.

### Establishment and evaluation of the NOA model in mice

Animal experiments were conducted after approval from the Animal Ethics Committee of College of Animal Science and Technology, Shihezi University. Animal experiments were performed according to ARRIVE guidelines.

Thirty-two male ICR mice (10 weeks old, $30.5 \pm 1.6$ g) were randomly divided into normal (n = 16) and NOA model groups (n = 16). Mice in the NOA model group

were injected intraperitoneally with leucovorin to simulate NOA in mice, at a dose of 40 mg/kg each, in 2 injections separated by 3 hours.

Based on the common clinical situation of NOA patients with a Johnsen score of 3 to 5, mice treated with leucovorin for 28 days were selected as the NOA disease model. At the same time, mice in the normal and NOA groups were mated 1:2 with female ICR mice (10 weeks old, 28.3 ± 1.1 g) to observe the litter size and further evaluate the effect of the NOA model.

Among the mice in the normal and NOA groups, 8 mice were randomly selected from each group, and after euthanasia by $CO_2$ asphyxiation, one side of the testis was rapidly collected for RT-qPCR assay, and the other side was used for Western blotting and model evaluation; the remaining 8 mice in the normal and NOA groups were mated 1:2 with female ICR mice in normal light, feeding, and watering environments, respectively, and the number of litters was counted.

**RT-qPCR validation of hub gene diagnostic efficiency**

Testicular samples were collected from both normal and NOA model groups. Total RNA was extracted using the TransZol Up Plus RNA Kit (ER501-01, TransGen Biotech), and cDNA synthesis was performed using the RevertAid First Strand cDNA Synthesis Kit (K1622, Thermo Fisher Scientific). Quantitative real-time PCR (qPCR) reactions were conducted with the SYBR Green I Master mix (04707516001, Roche). The expression of the seven hub genes was analyzed using the 2-ΔΔCt method. Primer sequences are listed in Supplementary Table 1.

**Western blotting**

The RIPA protein extraction reagent (50 mM Tris-HCl (pH 7.4), 150 mM NaCl, 1% NP-40, 0.1% SDS) was pre-cooled, the protease inhibitor Protease inhibitor cocktail (Roche, 04693116001) was added, and the testes were cut with surgical scissors for protein extraction. Protein concentration was determined by following the instructions of the BCA protein quantification kit (Cwbiotech, 02912E). Protein samples were adjusted to a consistent concentration, separated by SDS-PAGE, transferred to the membrane, and incubated with primary and secondary antibodies, respectively. The ECL droplets were added after exposure, development, and fixation. The images were analyzed in grayscale, using Gel Image ststem ver.4.00 (Tanon, China).

**Histologic examination of testes**

Testicular samples were dehydrated and fixed by gradient alcohol series, cleared by using xylene, embedded in paraffin, and sectioned at 5 μm. Sections were stained with hematoxylin and eosin and then observed under a light microscope (Nikon E100; Nikon) for model evaluation.

**Statistical analysis**

All statistical analyses were conducted in R (version 4.1.2). The Wilcoxon rank sum test was applied for the analysis of gene expression differences, with ROC curves assessing the diagnostic performance of key genes. Pearson correlation analysis elucidated relationships between hub genes and immune cell infiltration. The gene expression comparisons across groups were made by using Student's *t*-test.

## RESULTS

**Identification of differentially expressed genes (DEGs)**

We identified a total of 595 DEGs, with 532 genes being downregulated and 63 genes being upregulated in NOA cases. These results are visualized with a volcano plot (Figure 1A), and the top 10 upregulated and the top 10 downregulated DEGs are presented in a heatmap (Figure 1B).

**GO and KEGG enrichment analysis of spermatogenesis-related DEGs**

By overlapping the DEGs with spermatogenesis-related genes extracted from GO:0007283, we found 68 overlapped genes, namely spermatogenesis-related DEGs, depicted in a Venn diagram (Figure 2A).

The GO analysis revealed significant terms mainly associated with cellular processes involved in reproduction in multicellular organism, spermatid differentiation, and spermatid development (Figure 2B). The KEGG pathway analysis showed that the spermatogenesis-related DEGs were involved in pathways like endocrine and other factor-regulated calcium reabsorption, thyroid hormone synthesis, and gastric acid secretion (Figure 2C).

**PPI network construction and module analysis**

A PPI network of 68 spermatogenesis-related DEGs was generated by using the STRING database and visualized by Cytoscape (Figure 3A). Seven genes were selected as hub genes, using the MCODE plugin in Cytoscape, including CATSPER1, CATSPER3, CATSPER4, CATSPERG, OAZ3, ODF1, and SUN5 (Figure 3B).

**Evaluation of diagnostic performance of hub genes**

Expression analysis showed that all seven hub genes were downregulated in NOA compared to controls (Figure 4A). For ROC curve analysis, the AUC values of the 7 hub genes were determined to assess both the sensitivity and specificity of these genes in diagnosing NOA. ROC curve analysis revealed that each hub gene exhibited AUC values greater than 0.7, underscoring the high diagnostic potential for NOA (Figure 4B). To corroborate their diagnostic utility, an additional validation was performed using the GSE145467 dataset. Here, the seven hub genes maintained AUC values above 0.7, re

**Table 1. Statistics on the number of litters born to males and females in combined cages in the normal and NOA groups.**

| Treatment | | | | | |
|---|---|---|---|---|---|
| **Normal** | **Mated males** | **Mated females** | **Pregnant females** | **Conception rate (100%)** | **Number of litters** |
| **NOA** | **4** | **8** | **8** | **100** | **103** |
| | **4** | **8** | **0** | **0** | **0** |

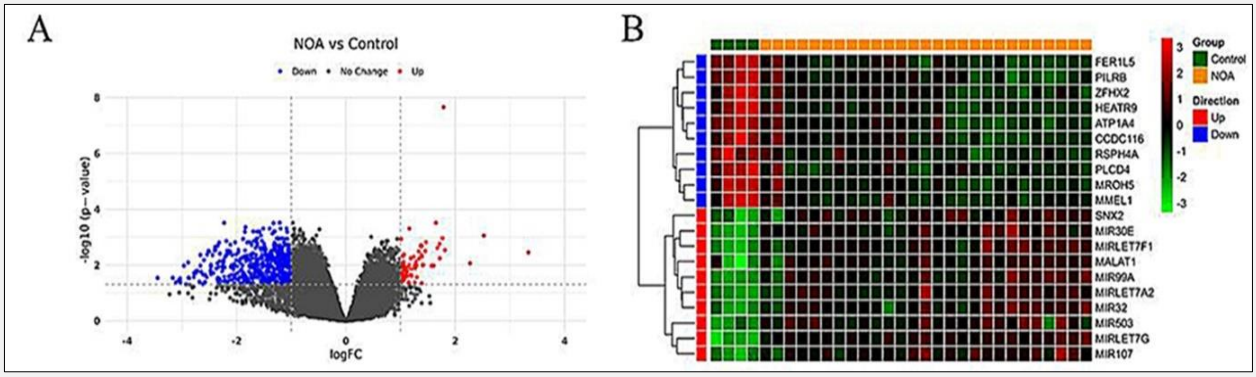


**Figure 1. A - The volcano plot of DEGs, B - The heatmap of the top 10 upregulated and top 10 downregulated DEGs.**

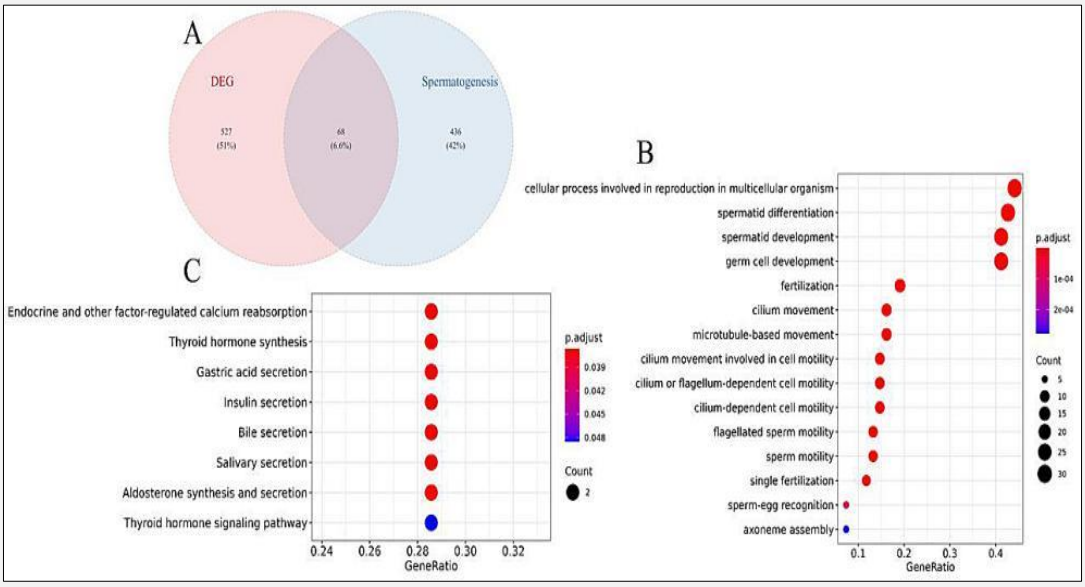


**Figure 2. A - The intersection of DEGs and spermatogenesis-related genes, B - GO enrichment analysis results of 68 spermatogenesis-related DEGs, C - KEGG enrichment analysis results of 68 spermatogenesis-related DEGs.**

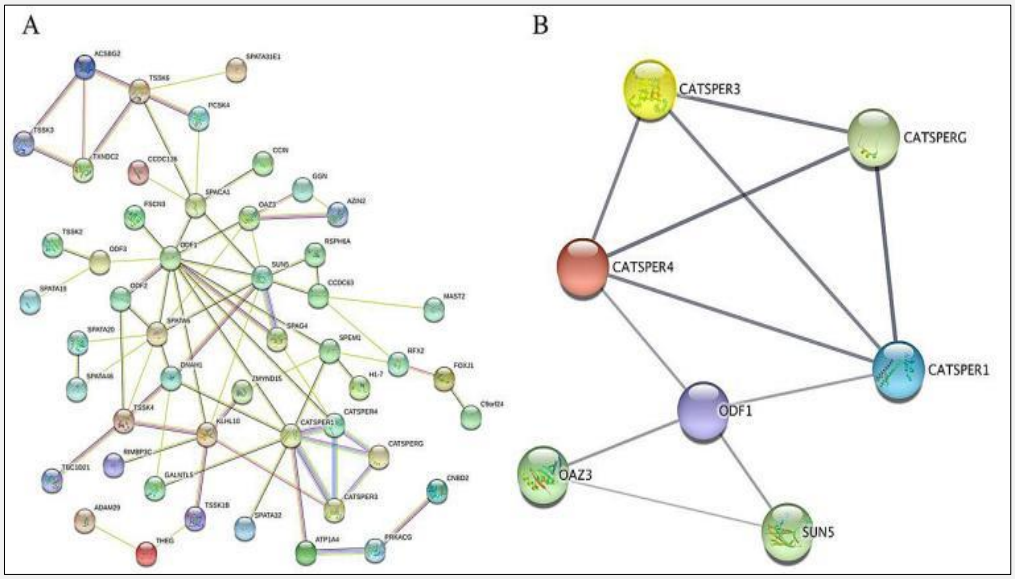


**Figure 3. A - The PPI network of 68 spermatogenesis-related DEGs, B - Hub genes in spermatogenesis-related DEGs.**

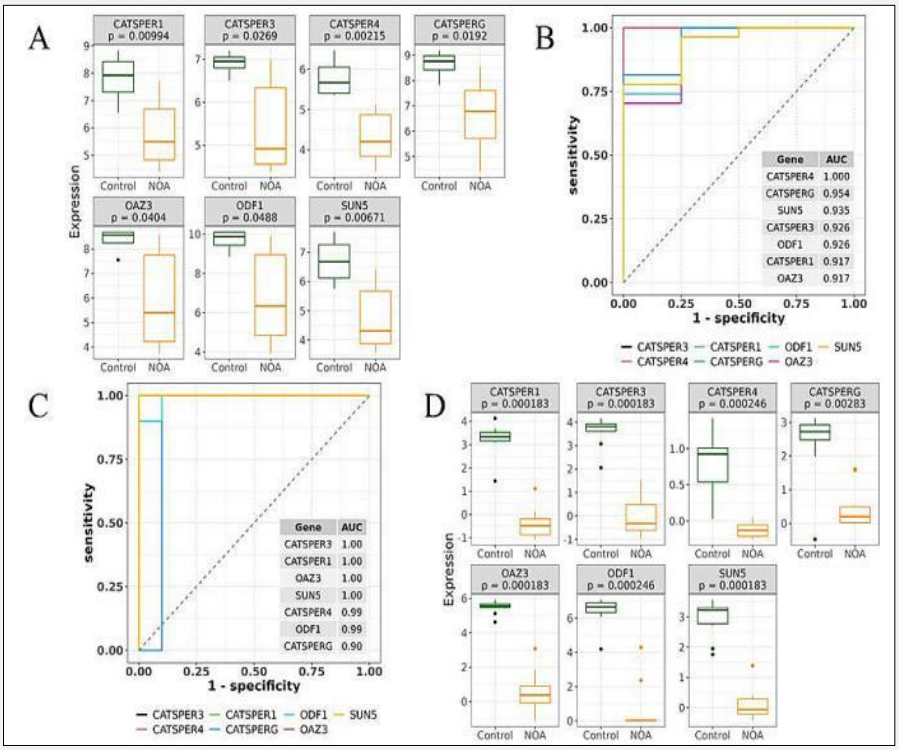


**Figure 4. A - The expression levels of 7 hub genes in NOA and control groups, B - The ROC analysis of the 7 hub genes, C - ROC analysis of the 7 hub genes in the GSE145467 dataset, D - The validation results of the expression levels of the 7 hub genes in the GSE145467 dataset.**

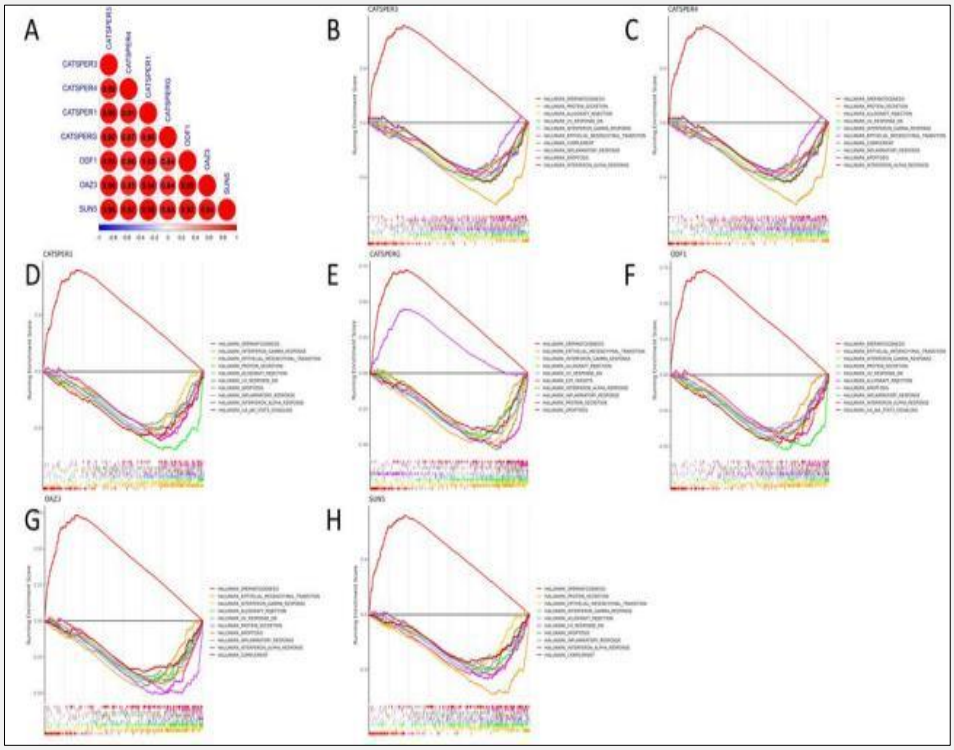


**Figure 5. A - The gene expression correlation analysis among the 7 hub genes, B - H - The GSEA analysis of the 7 hub genes.**

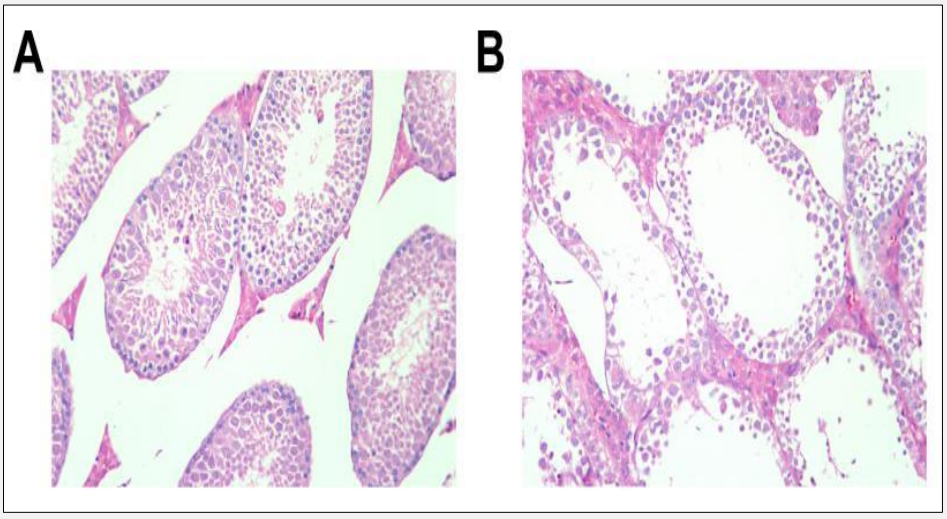


**Figure 6. A - Hematoxylin and eosin staining of seminiferous tubules in the normal group (magnification 200 µm), B – Hematoxylin and eosin staining of seminiferous tubules in the control group (magnification 200 µm).**

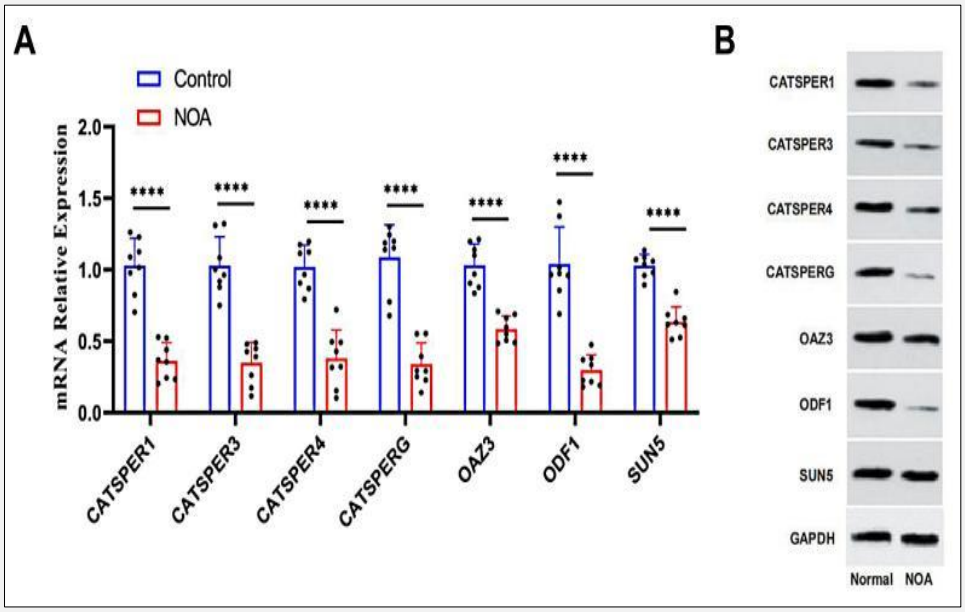


**Figure 7. Differential expression of 7 hub genes in normal and NOA groups.**

**A - The relative mRNA levels of CATSPER1, CATSPER3, CATSPER4, CATSPERG, OAZ3, ODF1, and SUN5 in the normal and mouse NOA model group, * p < 0.0001, B - The relative protein levels of CATSPER1, CATSPER3, CATSPER4, CATSPERG, OAZ3, ODF1, and SUN5 in the normal and mouse NOA model group, * p < 0.0001.**

inforcing their diagnostic significance for NOA (Figure 4C). In addition, similar expression patterns of those 7 hub genes were detected in GSE145467 (Figure 4D).

**Interaction effect and GSEA analysis for hub genes**

For a better understanding of interactions among these 7 hub genes, the correlation analysis was conducted. Correlation analysis showed strong interactions among the seven hub genes, with OAZ3 and ODF1 exhibiting the strongest correlation, followed by the correlation between SUN5 and CATSPER1 (Figure 5A).

GSEA was employed to elucidate the functional roles of our identified hub genes. The analysis revealed that genes with high-expression cohorts of these hub genes were significantly enriched in hallmark-spermatogenesis pathways, along with pathways associated with apoptosis and inflammatory response (Figure 5B-H).

**Construction of regulatory network of hub genes**

Utilizing the miRNet database and Cytoscape software, we constructed a network comprising 7 hub genes, 36 miRNAs, and 28 TFs. The network is visualized with diagnostic genes as blue squares, miRNAs as orange ovals, and TFs as purple diamonds (Supplementary Figure 1).

**Evaluation of mouse NOA model**

In the normal group, typical, normal spermatogenesis could be observed in the seminiferous tubules. In the NOA group, atrophy of the seminiferous tubules, absence of spermatozoa in the tubules, and significant reduction of spermatocytes could be observed, which conformed to the common clinical Johnsen scoring criteria of NOA (Figure 6); male rats in the NOA group had zero litters after mating with females, which is consistent with the clinical manifestations of NOA (Table 1).

**Expression changes of hub genes in a mouse model of NOA**

RT-qPCR and Western blotting analysis confirmed significant downregulation of CATSPER1, CATSPER3, CATSPER4, CATSPERG, OAZ3, ODF1, and SUN5 in the mouse NOA model compared to the normal group ($p < 0.0001$) (Figure 7).

## DISCUSSION

The clinical evaluation and treatment of NOA remains a formidable challenge, complicating the roles of healthcare practitioners and specialists in reproductive medicine. The advent of human-assisted reproductive tech-

nologies has underscored the importance of accurate NOA diagnosis, which is critical for guiding effective clinical interventions. Our study intersected 595 DEGs with known spermatogenesis-related genes. We obtained 68 spermatogenesis-related DEGs. Through comprehensive GO and KEGG enrichment analyses, we have delineated the enrichment of these DEGs in processes integral to multicellular organism reproduction, sperm differentiation, sperm development, and calcium reabsorption regulated by other factors. Previous studies [15] underscore the pivotal role of calcium ions ($Ca^{2+}$) in spermatocyte function, regulating sperm maturation, motility, the acrosome reaction, and fertilization. These $Ca^{2+}$ ions accumulate in spermatogenic cells at different stages of development and govern the process of spermatogenesis [16]. Disruptions in $Ca^{2+}$ signaling pathways may disrupt testosterone levels, leading to abnormal spermatogenesis and even complete male infertility.

To further identify the key genes affecting NOA, we constructed a PPI (protein-protein interaction) network and screened out seven hub genes (CATSPER1, CATSPER3, CATSPER4, CATSPERG, OAZ3, ODF1, and SUN5). The results of ROC analysis indicated that these seven hub genes have significant diagnostic value for NOA. Notably, the CATSPER family genes (CATSPER1-4) are known to form alkalization-activated $Ca^{2+}$ permeable channels and play crucial roles in sperm motility, the acrosome reaction, and sperm-oocyte fusion [17]. Among them, the CATSPER1, CATSPER2, and CATSPER3 proteins have strong interactions with glycolytic proteins (such as GAPDHS and PGK2), while the CATSPER4 protein is strongly associated with the function of the sperm flagellum [18]. In mouse sperm, knocking out the CATSPER1 gene can affect the formation of $Ca^{2+}$ channels [19], thereby impacting the fertilization ability of mouse sperm. However, the expression of CATSPER1 depends on Sox transcription factors, which possess a calmodulin-binding domain for nuclear transport. When calmodulin (CaM) is inhibited by a specific inhibitor (calmidazolium, CMZ), it can prevent the nuclear transport of Sox factors, subsequently disrupting the expression and production of CATSPER1. This may prevent the formation of functional CATSPER channels, which are located in the flagella of sperm cells and are necessary for alkaline depolarization and cyclic nucleotide-activated $Ca^{2+}$ influx. Consequently, this can affect sperm hyperactivation and motility. The mRNA expression of CATSPER1 and CATSPER3 is negatively correlated with sperm DNA fragmentation, indicating that lower levels of CATSPER1 and CATSPER3 mRNA are associated with poor sperm quality [20]. CATSPERG is a single transmembrane protein related to the CATSPER complex, with a large extracellular domain and a short intracellular tail. CATSPERG mRNA is detected only in the testis, and its expression pattern is highly similar to CATSPER1-4. CATSPERG is localized to the principal piece of the sperm, and its trafficking and assembly depend on CATSPER1. Therefore, in the absence of CATSPER1 in sperm, CATSPERG protein (but not the K+ channel protein KCNU1) is also deficient [21].

OAZ3, a member of the OAZ gene family, is specifically expressed in germ cells and regulates the concentration of polyamines within the cell. A study has found that OAZ3, along with GGNBP1, GGNBP2, and GGN1, is involved in the development of male germ cells [22]. By controlling the key enzymes involved in polyamine biosynthesis, it regulates the concentration of polyamines in the body. Large amounts of polyamines are synthesized and stored in the testes, and they affect cell proliferation and differentiation by binding to nucleic acids as cations [23].

Normal sperm morphology and motility are pivotal for successful fertilization. During spermatogenesis, the tight association between the sperm head-tail connector and the nuclear membrane is crucial for ensuring sperm capacitation and the integrity of fertilization [24]. ODF1 is the major protein of the outer dense fibers in the tail of mammalian sperm. The development of the sperm flagellum originates from centrioles migrating from the nucleus's anterior to its posterior, establishing sperm bipolarity through the positioning of the acrosome and flagellum [25]. These centrioles are integral not only to flagellum formation but also to the creation of a complex structure at the nuclear indentation known as the implantation fossa. This structure, the connecting piece, ensures the head and tail are firmly joined, a vital factor for sperm's progressive motility and the nuclear transfer to the oocyte during fertilization [26,27]. ODF1 protects the sperm tail from shear forces by maintaining flagellar elasticity during epididymal transport and ejaculation. When male mice lack ODF1, although there are no obvious structural abnormalities, there are no intact sperm in the epididymis, indicating that the head and tail are not properly connected. Moreover, disruptions in this connectivity due to ODF1 absence were observed, with applied force leading to head-tail separation [28].

Previous studies have shown that SUN5 interacts with ODF1, SUN5 interacts with Nesprin3, and ODF1 interacts with Nesprin3, forming a "triplet" structure through interactions in the neck region of the sperm. When gene mutations lead to the loss of SUN5, the "triplet" structure disappears and the head-tail connection becomes fragile, leading to the occurrence of acrosomeless sperm syndrome (ASS) [29]. ASS, a rare genetic reproductive disorder, is associated with SUN5 mutations in approximately 33 - 47% of cases, though the underlying molecular mechanisms remain unclear [30]. Studies involving SUN5 gene knockout mice mirrored the head-tail disconnection akin to human ASS, accompanied by a decrease in sperm-related proteins ODF1 and ODF2. Further, it was demonstrated that SUN5 and Nesprin3 contribute to forming a linker of the nuclear lamina and cytoskeletal (LINC) complex, crucial for the head-tail linkage. Notably, in SUN5 knockout mice, Nesprin3's localization at the implantation fossa is disrupted, misplacing the centriole and leading to head-tail separation

[31]. Therefore, it is believed that the interaction between SUN5, Nesprin3, and ODF1 is one of the reasons for the impaired head-tail connection in sperm.
This study also explored the expression correlations among seven hub genes, identifying strong associations between SUN5 and CATSPER1 and between ODF1 and OAZ3. GSEA analysis of these genes highlighted their significant enrichment in spermatogenesis markers, suggesting their potential role in regulating NOA through aspects such as glycolysis, sperm head-tail connection, and tail motility. Nonetheless, targeted disruption of channel genes in mice did not yield significant male fertility defects, indicating a need for further studies to evaluate the functional roles of CATSPERG and others within this context.

## CONCLUSION

In summary, this study identified seven key genes associated with spermatogenesis, offering novel insights into the molecular underpinnings of NOA. These findings present a solid foundation for developing potential bio markers and therapeutic targets, thereby enhancing the diagnosis, treatment, and monitoring of NOA patients.

**Source of Funds:**
Research and Application of Gender Control in Tarim Red Deer (no. KH0069).
Key Project of Shihezi University Provincial Science and Technology Innovation (grant no. 2020SK1013).

**Data Availability Statement:**
Microarray expression data for NOA and controls were downloaded from the Gene Expression Omnibus (GEO) database (GSE45885 and GSE145467). The GSE45885 dataset consists of 27 NOA samples and 4 controls and was used as training set. The GSE145467 dataset consists of 10 NOA samples and 10 controls and was used as validation set. The list of spermatogenesis-related genes was obtained from GO:0007283 in GO database.

**Ethical Approval Statement:**
All animal experiments were complied with the ARRIVE guidelines and performed in accordance with the National Institutes of Health Guide for the Care and Use of Laboratory Animals. The experiments were approved by the institutional Animal Care and Use Committee of College of Animal Science and Technology, Shihezi University (no. 2021-XJ414 ).

**Declaration of Interest:**
The authors have no conflicts of interest to declare.

**References:**

1. Olesen IA, Andersson A-M, Aksglaede L, et al. Clinical, genetic, biochemical, and testicular biopsy findings among 1,213 men evaluated for infertility. Fertil Steril 2017;107(1):74-82.e7. (PMID: 27793385)

2. Ghanem M, Bakr NI, Elgayaar MA, El Mongy S, Fathy H, Ibrahim A-HA. Comparison of the outcome of intracytoplasmic sperm injection in obstructive and non-obstructive azoospermia in the first cycle: a report of case series and meta-analysis. Int J Androl 2005;28(1):16-21. (PMID: 15679616)

3. Liu L, Li F, Wen Z, et al. Preliminary investigation of the function of hsa_circ_0049356 in nonobstructive azoospermia patients. Andrologia 2020;52(11):e13814. (PMID: 32894622)

4. Majzoub A, Arafa M, Khalafalla K, et al. Predictive model to estimate the chances of successful sperm retrieval by testicular sperm aspiration in patients with nonobstructive azoospermia. Fertil Steril 2021;115(2):373-81. (PMID: 33059887)

5. Yatsenko AN, Georgiadis AP, Röpke A, et al. X-linked TEX11 mutations, meiotic arrest, and azoospermia in infertile men. N Engl J Med 2015;372(22):2097-107. (PMID: 25970010)

6. Cioppi F, Rosta V, Krausz C. Genetics of Azoospermia. Int J Mol Sci 2021;22(6):3264. (PMID: 33806855)

7. Xie C, Chen X, Liu Y, Wu Z, Ping P. Multicenter study of genetic abnormalities associated with severe oligospermia and nonobstructive azoospermia. J Int Med Res 2018;46(1):107-14. (PMID: 28730893)

8. The Gene Ontology Consortium. Expansion of the Gene Ontology knowledgebase and resources. Nucleic Acids Res 2017; 45(D1):D331-8. (PMID: 27899567)

9. Kanehisa M, Goto S. KEGG: kyoto encyclopedia of genes and genomes. Nucleic Acids Res 2000;28(1):27-30. (PMID: 10592173)

10. Szklarczyk D, Franceschini A, Wyder S, et al. STRING v10: protein-protein interaction networks, integrated over the tree of life. Nucleic Acids Res 2015;43(Database issue):D447-52. (PMID: 25352553)

11. Shannon P, Markiel A, Ozier O, et al. Cytoscape: a software environment for integrated models of biomolecular interaction networks. Genome Res 2003;13(11):2498-504. (PMID: 14597658)

12. Bader GD, Hogue CWV. An automated method for finding molecular complexes in large protein interaction networks. BMC Bioinformatics 2003;4:2. (PMID: 12525261)

13. Robin X, Turck N, Hainard A, et al. pROC: an open-source package for R and S+ to analyze and compare ROC curves. BMC Bioinformatics 2011;12:77. (PMID: 21414208)

14. Fan Y, Xia J. miRNet-Functional Analysis and Visual Exploration of miRNA-Target Interactions in a Network Context. Methods Mol Biol 2018;1819:215-33. (PMID: 30421406)

15. Cui Z, Agarwal A, da Silva BF, Sharma R, Sabanegh E. Evaluation of seminal plasma proteomics and relevance of FSH in identification of nonobstructive azoospermia: A preliminary study. Andrologia 2018;50(5):e12999. (PMID: 29528137)

16. Bai G, Zhai X, Liu L, et al. The molecular characteristics in different procedures of spermatogenesis. Gene 2022;826:146405. (PMID: 35341953)

17. Shur BD, Rodeheffer C, Ensslin MA. Mammalian fertilization. Curr Biol 2004;14(17):R691-2. (PMID: 15341754)

18. Zhang X, Huang R, Zhou Y, Zhou W, Zeng X. IP3R Channels in Male Reproduction. Int J Mol Sci 2020;21(23):9179. (PMID: 33276427)

19. Ren D, Navarro B, Perez G, et al. A sperm ion channel required for sperm motility and male fertility. Nature 2001;413(6856):603-9. (PMID: 11595941)

20. Maurya S, Bhoi NR, Kesari KK, Roychoudhury S, Kumar D. In Silico Analysis of CatSper Family Genes and APOB Gene Regulation in Male Infertility. Adv Exp Med Biol 2022;1391:323-32. (PMID: 36472830)

21. Forero-Forero A, López-Ramírez S, Felix R, et al. Down Regulation of Catsper1 Expression by Calmodulin Inhibitor (Calmidazolium): Possible Implications for Fertility. Int J Mol Sci 2022; 23(15):8070. (PMID: 35897646)

22. Jalalabadi FN, Cheraghi E, Janatifar R, Momeni HR. The Detection of CatSper1 and CatSper3 Expression in Men with Normozoospermia and Asthenoteratozoospermia and Its Association with Sperm Parameters, Fertilization Rate, Embryo Quality. Reprod Sci 2024;31(3):704-13. (PMID: 37957468)

23. Wang H, Liu J, Cho K-H, Ren D. A novel, single, transmembrane protein CATSPERG is associated with CATSPER1 channel protein. Biol Reprod 2009;81(3):539-44. (PMID: 19516020)

24. Zhang J, Wang Y, Zhou Y, Cao Z, Huang P, Lu B. Yeast two-hybrid screens imply that GGNBP1, GGNBP2 and OAZ3 are potential interaction partners of testicular germ cell-specific protein GGN1. FEBS Lett 2005;579(2):559-66. (PMID: 15642376)

25. Tokuhiro K, Isotani A, Yokota S, et al. OAZ-t/OAZ3 is essential for rigid connection of sperm tails to heads in mouse. PLoS Genet 2009;5(11):e1000712. (PMID: 19893612)

26. Liu R, Qu R, Li Q, et al. ARRDC5 deficiency impairs spermatogenesis by affecting SUN5 and NDC1. Development 2023; 150(24):dev201959. (PMID: 37997706)

27. Fawcett DW. The mammalian spermatozoon. Dev Biol 1975; 44(2):394-436. (PMID: 805734)

28. Mortimer D. The functional anatomy of the human spermatozoon: relating ultrastructure and function. Mol Hum Reprod 2018; 24(12):567-92. (PMID: 30215807)

29. Chemes HE, Rawe VY. The making of abnormal spermatozoa: cellular and molecular mechanisms underlying pathological spermiogenesis. Cell Tissue Res 2010;341(3):349-57. (PMID: 20596874)

30. Hoyer-Fender S. Development of the Connecting Piece in ODF1-Deficient Mouse Spermatids. Int J Mol Sci 2022;23(18):10280. (PMID: 36142191)

31. Zhang D, Huang W-J, Chen G-Y, et al. Pathogenesis of acephalic spermatozoa syndrome caused by SUN5 variant. Mol Hum Reprod 2021;27(5):gaab028. (PMID: 33848337)

**Additional material can be found online at:**
http://supplementary.clin-lab-publications.com/240541/